# Phase response curves in the characterization of epileptiform activity

J. L. Perez Velazquez,[1,2] R. F. Galán,[3] L. Garcia Dominguez,[1] Y. Leshchenko,[1] S. Lo,[1] J. Belkas, and R. Guevara Erra[1]
[1]*Brain and Behaviour Programme, Neurosciences & Mental Health Programme, Hospital for Sick Children, Toronto M5G1X8, Canada*
[2]*Department of Paediatrics and Institute of Medical Science, University of Toronto, Toronto M5G1X8, Canada*
[3]*Department of Biology, Carnegie Mellon University and Centre for the Neural Basis of Cognition, Pittsburgh, USA*
(Received 13 August 2007; published 19 December 2007)

Coordinated cellular activity is a major characteristic of nervous system function. Coupled oscillator theory offers unique avenues to address cellular coordination phenomena. In this study, we focus on the characterization of the dynamics of epileptiform activity, based on some seizures that manifest themselves with very periodic rhythmic activity, termed absence seizures. Our approach consists in obtaining experimentally the phase response curves (PRCs) in the neocortex and thalamus, and incorporating these PRCs into a model of coupled oscillators. Phase preferences of the stationary states and their stability are determined, and these results from the model are compared with the experimental recordings, and interpreted in physiological terms.

DOI: 10.1103/PhysRevE.76.061912 PACS number(s): 87.19.La, 05.45.Xt

## I. INTRODUCTION

Recent years have witnessed a surge of interest in the concept that synchronized activity in brain cellular networks plays a crucial role in information processing and behavioral responses [1,2]. However, adequate frameworks to understand the relation between brain function and behavior are still underdeveloped. The theory of coupled oscillators [3] offers a very adequate level of description to study the dynamics of coordinated activity in neuronal ensembles, and to characterize the functional connectivity between brain areas that is being sought intensively these days in efforts to investigate how specific brain activities associate with behavioral responses [4,5]. In general, these coupled oscillator models require setting up differential equations that describe the time evolution of parameters of the system; a main problem applying these analyses to biological activity is that realistic and accurate model equations are not trivial to obtain from experimental data [6–8].

In this study, we focus on the characterization of the dynamics of epileptiform activity, based on some seizures that manifest themselves with very periodic rhythmic activity termed absence seizures, and more specifically in this case, spike and wave discharges (SWDs). This activity is restricted to the thalamus and neocortex [9,10]; thus, the rhythmic paroxysmal activity can be thought of as a manifestation of the activity of two coupled oscillators: the thalamus and the cortex; and the relative stability of the SWD oscillation can be represented by an asymptotic stable limit cycle in the thalamocortical activity [11]. It is known that when coupled limit cycle oscillators are weakly perturbed, the system can be reduced to a phase model [12–14]. Phase models contain terms that represent the interaction function between the oscillators. Hence, our approach consists in obtaining experimentally the phase resetting curves (PRCs) in the neocortex and thalamus, and incorporating these PRCs into a phase model of coupled oscillators as the interaction functions. Phase differences between neurophysiological recordings is an adequate order parameter [15] to describe temporal relations between brain areas and to catch a glimpse of the establishment of their possible functional connectivity. We exploit the PRC as a tool to understand coordinated brain activity, as it represents a natural approach to characterize neuronal interactions [3,14,16,17]. PRCs have been used to analyse synchronization properties of natural [18–21] and artificial neural systems [22]. PRCs describe the alteration of the phase due to an input at each point of the cycle, and therefore the reconstruction of a PRC requires sustained periodic activity. We thus take advantage of the robust periodic paroxysmal activity representing the SWD, which makes the reconstruction of a PRC simpler than in other systems and situations where the rhythmic activity is not that robust. The terms "resetting" and "response" are normally used interchangeably, nevertheless, in our experimental situation here described, the term "response" is probably more adequate (a more detailed discussion of this issue can be found in Ref. [23]). After deriving PRCs in the thalamus and neocortex, we incorporate these into a model of coupled oscillators, representing the time evolution of the respective phases and of their phase difference, to assess stable phase locking patterns in the activity of these two brain areas.

## II. METHODS

### A. In vivo intracerebral recordings

Bipolar electrodes (Plastics One, Roanoke, Virginia, USA) were implanted chronically into specific brain areas of Wistar rats (50–60 days old) using a stereotaxic apparatus. The stereotaxic coordinates of electrode implantation were: into the thalamus B-2.1, ML −1.4, D 6.4 and into cortex B −0.4, ML +/−3.0, D 2.0 (see Fig. 1 for a schematic of electrode placement). The electrode leads were fixed to the skull using dental acrylic and three screws attached to the parietal regions of the scalp. After a recovery period of ~5 days, animals were placed in an electrically screened Plexiglass chamber for recordings. The recording electrodes were connected to an AI 402×50 Ultralow noise differential amplifier (Axon instruments, Foster City, California, USA), a CyberAmp380 signal conditioner (Axon instruments), and a digital converter MP150 (Biopac, Harvard Instruments, St. Laurent, Quebec, Canada). Recordings were acquired at 1000 Hz.

 

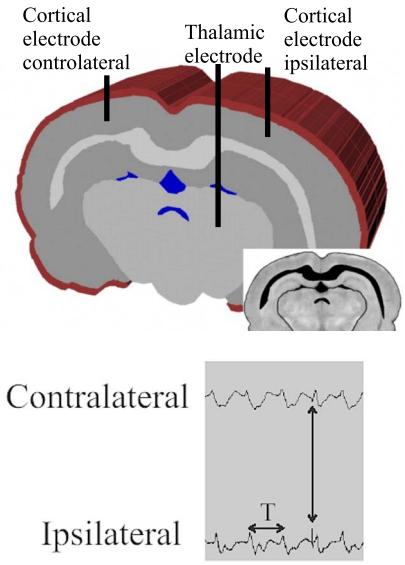


FIG. 1. (Color online) Anatomical location of the recording/stimulating electrodes in the rat brain. The thalamic or the cortical (ipsilateral) electrode was stimulated while the brain activity had spike and wave seizures (SWD) shown below. Traces show a fragment of a seizure recorded simultaneously in both cortical electrodes and the stimulating artifacts (arrow) after a single thalamic stimulation. *T* denotes the period of the SWD.

When needed, intracerebral stimulation was generated with a Grass square pulse stimulator S88K (Grass Instruments) equipped with a stimulation isolation unit, that delivered square current pulses (0.1 ms) in the range 0.1 $\mu$A to 15 mA. Since our electrodes can be used as recording or stimulating leads, only one electrode was inserted into each area. This arrangement also allowed us to record simultaneously from the thalamus and cortex when needed (see Fig. 4, for example). Initial electrophysiological data processing was done using the software package ACKNOWLEDGE (Biopac, Harvard Instruments).

### B. Absence seizure models

To calculate the phase response curves we took advantage of the very periodic rhythms observed in two seizure models that are considered to represent human absence epileptiform activity. The first model of typical absence seizures is induced in rats as previously described [9]. Briefly, animals were administered 100–120 mg/kg of $\gamma$-butyrolactone (GBL) via intraperitoneal injection, and intracerebral electrophysiological recordings were obtained for a period of 2–4 h thereafter. Shortly after GBL injection (3–5 min), absence seizures were recorded from thalamus and cortex, consisting of bilaterally synchronous spike and wave discharges (SWD, Figs. 1 and 2), with mean frequency of ~4 Hz. The second model is a chronic model of absence seizures, induced by treatment with the cholesterol synthesis inhibitor AY9944 (7.5 mg/kg), every 6 days from postnatal day 2 to 20, as described in detail previously [24]. This treatment promotes chronic SWD paroxysmal activity that can be recorded from thalamus and cortex, with mean frequency of ~8 Hz. These

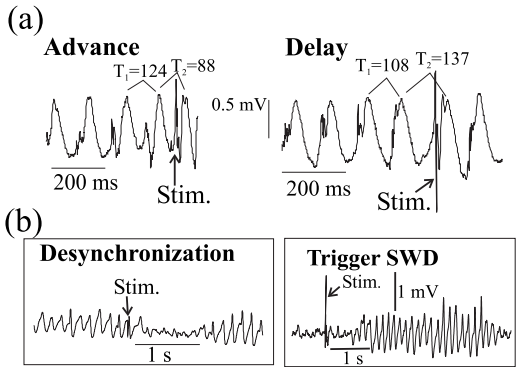


FIG. 2. Experimental recordings in the cortex of SWDs showing the results of a single pulse delivered in the thalamus. (a) $T_1$ and $T_2$ are the periods of the oscillation preceding and just after the single pulse (stim.) respectively, and the duration is shown in milliseconds. The recordings come from two different rats. (b) Sometimes, a momentary halting of the spike and wave was noted after the perturbation (left trace), but there was no specific phase for the perturbation to cause the transitory desynchronization (see text for more details). The right-hand side recording depicts an instance when the single pulse delivered into the thalamus triggered a SWD recorded in the cortex. This effect was dependent upon the behavioral state of the animal as discussed in Sec. III.

seizures last throughout the life of the animal, and therefore it is a chronic model. The exact mechanisms by which these drugs induce seizures are still under scrutiny; GBL is thought to mediate the induction of oscillations via modulation of $GABA_B$ receptors in the thalamic cells, therefore increasing the probability of synchronous activity in the thalamus. Manipulations of the rats were performed according to the protocols approved by the Animal Care Committee of the Hospital for Sick Children.

### C. Data analysis

To estimate the cortical and thalamic phase response curves (PRC), a single, "weak" stimulus was applied to the thalamus or cortex, while recording from cortex or thalamus, respectively. Normally, two amplitudes of stimulation were used, one weak and another "strong" which always produced a local field response reflected as a spike-and-wave (hence, this latter input produced a straight line in the PRC plot). The weak input was used to estimate the PRC, since the frameworks of coupled oscillators require weakly connected units [12]. The stimulation was done at random times, making sure there were at least 3–4 s in between stimuli to allow a few cycles in the SWD. In this study, we follow Winfree [3] and define phase as the time between an arbitrary reference (which in our cases can be either the stimulating artefact or the next spike in the waveform) divided by the period. As a result of this weak perturbation, the next wave could be advanced, delayed, or unchanged, as shown in Fig. 2. The intracerebral stimulation was generated with a Grass square pulse stimulator S88K (Grass Instruments) equipped with a stimulation isolation unit, that delivered square current pulses in the range 0.1 $\mu$A to 15 mA. The duration of the pulse was set to 0.1 ms. The phase shift after the perturba-

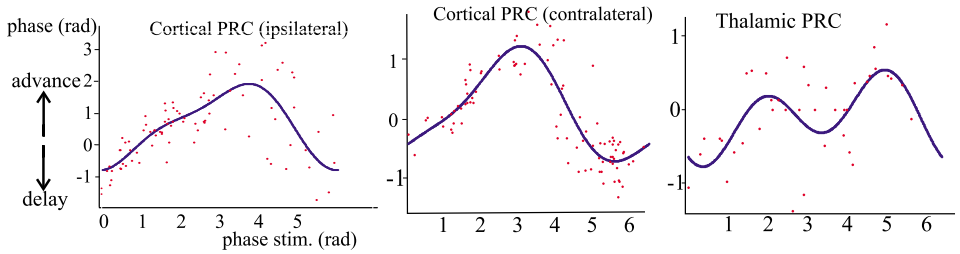


FIG. 3. (Color online) The experimentally obtained PRCs, for the cortex in both sides ipsilateral and contralateral (in response to thalamic stimulation) and thalamus (cortical stimulation), were approximated by a Fourier series, represented by the blue curve. The cortical PRCs are derived from one rat, and the thalamic from another (GBL injected).

tion, used to estimate the PRC, was calculated using the periods of the oscillation [see Fig. 2(a), and Ref. [17]] and the following formula [17]:

$$\theta = \frac{T_1 - T_2}{T_1} \times 2\pi.$$

$T_1$ and $T_2$ are the periods of the oscillation preceding and just after the single pulse, respectively, and the multiplication by $2\pi$ is used to convert it to radians. In this fashion, a positive phase shift ($T_1 > T_2$) indicates an advance of the next spike in the waveform [as shown in Fig. 2(a)]. The graph of this function $\theta$ is the PRC. The values shown in the figures correspond to individual rats and are not averaged except for those points that fell on the same phase of the perturbation.

In this study we follow the philosophy of the Kuramoto model, since we describe the brain areas that oscillate (thalamus and cortex) as phase oscillators that are deterministically coupled. This allows us to calculate stable phase-locked states and compare them with the values obtained experimentally. A complementary approach could be applied to take into account the natural phase variability explicitly, i.e., to investigate stochastic synchronization [25]. However, due to the high regularity of the signals during the seizure, we focus here on the deterministic Kuramoto model.

## III. RESULTS

To derive the PRCs we used only those recordings that were very periodic, so that the estimation of the period was as clear as possible. Our criterion was that the values of each period was within ~10% of the average, that is, we accepted values of, for example, 124±12 ms (this for the AY9944-induced seizures with average frequency of 7–8 Hz). Thus, of 42 rats recorded, only 17 were used to estimate the PRC because seizures in these animals had our required periodicity to derive the PRC. To estimate the cortical and thalamic PRC, a single, "weak" stimulus was applied to the thalamus or cortex respectively. When stimulating the thalamus, two cortical recordings were simultaneously obtained, from the ipsilateral and contralateral side (Fig. 1), in order to see possible differences in the PRC derived from a unilateral thalamic stimulation. The PRCs were qualitatively the same in both cortical hemispheres (Fig. 3). By "weak" stimuli is meant that the amplitudes of the single pulses delivered through the stimulating electrode were the minimal (which varied from rat to rat, but were in the range of 10 $\mu$A–1 mA) that allowed an identification of the stimulating artifact (so that the phase of the stimulation could be calculated) and did not alter the oscillation. Thus, two amplitudes of stimulation were used, one weak and another "strong" (normally >10 mA), the latter always produced a local field potential response which was manifested as a spike-and-wave, hence, this input obviously produced a straight line when constructing the PRC (data not shown) and thus these were not used in the analysis. The weak input was used to estimate the PRC. As a result of this weak perturbation, the next wave in the SWD could be advanced, delayed, or unchanged (Fig. 2). It is noteworthy that, when using the larger stimulating amplitudes, we sometimes found that the single pulse was able to halt momentarily the SWD, as depicted in Fig. 2(b). Only brief (~1 s) stopping (desynchronization) of the SWD was observed in 55% of the stimulations at large stimulation intensities. Because this phenomenon may depend on the phase at which the perturbation is applied, we calculated the phase of the single applied pulses in these cases that led to transitory desynchronization. However, no specific phase of the perturbation was noted. Another interesting observation relates to the low threshold that these rats have for triggering a SWD [24], as shown in Fig. 2(b), and the question arises as to whether there is a particular phase at which the single pulse can trigger the SWD. This phenomenon occurred in 53% of stimulations when the rats were exploring, and in 86.1% when the rats were resting; thus, this phenomenon is dependent on the state of the animal. The instantaneous phase at which a single pulse triggered a seizure was evaluated, but in this case we had to extract the instantaneous phase using the Hilbert transform because, obviously, there was no SWD before the stimulation [Fig. 2(b)]. This process requires the use of band-passed signals [25], therefore in our analysis we focused on the range 12 to 30 Hz, using a band pass of ±2 Hz. Just as in the above case of seizure abortion, no particular instantaneous phase was noted in the pulses that triggered a SWD. Hence, it seems that the perturbation can be applied at any phase of the oscillation to stop or start the rhythm in these rats, the only requirement is to be of sufficient amplitude.

Figure 3 depicts three PRCs obtained from the simultaneous cortical recordings (ipsilateral and contralateral sides) in response to thalamic stimulation, and from the thalamic recordings (ipsilateral) in response to cortical stimulation. The cortical PRCs in the figure correspond to one rat, and the thalamic PRC to a different animal. As shown in the figure,

the ipsilateral and contralateral cortical PRCs were qualitatively similar, most of the stimulation causing an advance of the wave (positive phase values, as detailed in Sec. II indicate advancement). Qualitatively, this form of the PRC was observed in 7 of 11 rats in which the cortical PRCs were evaluated, while in the other four rats the PRC was a straight horizontal line, indicating that the perturbation was too small to induce any phase shift. The thalamic PRC indicated an advancement of the wave when the cortex was stimulated in the middle of the oscillation period, while for other phases of stimulation the PRC remained around 0 or became negative, thus delaying the next wave (Fig. 3). This thalamic PRC was observed in five of six rats. No differences in the PRCs were noted between the two rat absence seizure models described in methods, those caused by injection of GBL or the SWD resulting from AY9944 treatment. This is expected as both models results in SWD in the thalamocortical system, the main difference being the frequency of the oscillation: ~4 Hz after GBL administration and ~8 Hz after AY9944 injections.

We then approximated the PRCs with a Fourier series (blue lines in Fig. 3), and inserted these into the following coupled oscillator model of the Kuramoto type:

$$\frac{d\theta_c}{dt} = \omega_c + K_{tc}H_c(\theta_c - \theta_t),$$

$$\frac{d\theta_t}{dt} = \omega_t + K_{ct}H_t(\theta_t - \theta_c),$$

where $\theta_c$ and $\theta_t$ are the phases of the cortex and thalamus respectively, $K_{tc}$ and $K_{ct}$ are the couplings between thalamus and cortex (thalamocortical) and between cortex and thalamus (corticothalamic), $H$ is the interaction function (in our case it is the calculated PRC, if we assume fast interactions compared with the period of the oscillation, which is true for synaptic transmission; see Sec. IV for more detailed comments on this point), $\omega$ are the intrinsic frequencies that in the case of GHB-induced seizures was taken 4 Hz (and ~8 Hz for AY9944-injected rats), the frequency of the SWD. To calculate the fixed phase differences ($\Delta\theta = \theta_t - \theta_c$), that is, the stationary states of phase locking, the equations are subtracted

$$\frac{d\Delta\theta}{dt} = \Delta\omega + K_{ct}H_t(\Delta\theta) - K_{tc}H_c(-\Delta\theta)$$

and solved for $\frac{d\Delta\theta}{dt}=0$ to reveal stationary states of the phase difference $\Delta\theta_0$. The stability of the stationary states is then determined by the slope of $\frac{d\Delta\theta}{dt}$ at the stationary state $\Delta\theta_0$, if $\frac{d}{d\Delta\theta}\left(\frac{d\Delta\theta}{dt}\right)|_{\Delta\theta_0} < 0$ the stationary state is stable. We approximated the experimentally obtained interaction function ($H(\theta)$) with a Fourier series

$$H = \sum_{n=0}^{2} a_n \cos(n\theta) + \sum_{n=0}^{2} b_n \sin(n\theta).$$

The approximation used the first three Fourier components:

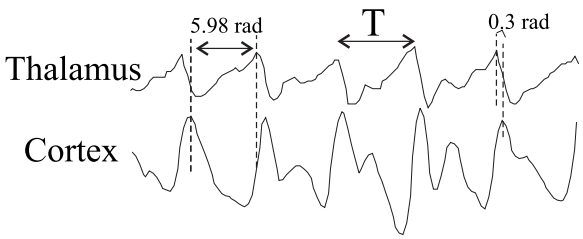


FIG. 4. Experimental simultaneous recording in the thalamus and cortex during an SWD, depicting the phase difference between the oscillations, approximately 240 ms, 5.98 rad (or ~12 ms, 0.3 rad, if we consider the smaller time lag between spikes) for SWD induced by GBL that have a period of ~250 ms (see Sec. II),

$$H(\theta) = a_0 + a_1 \cos\theta + a_2 \cos(2\theta) + b_0 + b_1 \sin\theta + b_2 \sin(2\theta).$$

As mentioned above, PRCs, were derived from several rats for the ipsilateral and contralateral cortical sites and the thalamic site (Fig. 3), but, by varying the Fourier coefficients, the general form of the equations was able to fit any of the measured PRC. Solving the system for $\omega_c$ and $\omega_t = 4$ and the coupling factors ($K_{tc}$ and $K_{ct}$) initially set to 1 (symmetric) for simplicity, two stationary states were found: one was centered around 6.18 rad in case of the system thalamus-ipsilateral cortex, and 5.75 rad for the system thalamus-contralateral cortex. These were stable stationary states. Another stationary state was found at 4.18 rad (thalamus-ipsilateral) and 4.64 (thalamus-contralateral), but these were unstable. We then compared the stable phase difference with that found in the experimental recordings, which had an average of 342±10° (5.98±0.17 rad, or ~237 ms considering 4 Hz the frequency of the SWD); one example is depicted in Fig. 4. In general, in rhythmic oscillations, it is not very meaningful to state that one oscillator leads the other, as this is a matter of the reference we take. At least, in our recordings, we can determine in which electrode the spike-and-wave starts, and while there is some variability, the first spike is observed in the thalamus in 20-30% of the times. Table II reveals that there is a stable state of 0.45 rad (17 ms) for $K_{ct}=0.5$ and $\Delta\omega=0$. With these parameters, the model optimally reproduces the phase difference observed experimentally. Hence, a look at Fig. 4 thus reveals a small lag between the spike in the thalamus and in the cortex ~0.3 rad (that is $2\pi - 5.98$, or ~12 ms). We note that this relatively small phase difference could be due to conduction delays between the cortex and thalamus. Considering that there is a monosynaptic connection between these two areas (more specifically, between the ventrobasal thalamic nucleus, where our thalamic electrode was inserted, and layer IV of the cortex, where the cortical electrodes were placed), that the distance between electrodes (thalamus-ipsilateral cortex) is ~4.4 mm, and taking values of axonal conduction velocity between 2.3 and 17 m/s, as observed in rat cortico-spinal axons, a conduction delay between 1.9 and 0.26 ms is conceivable. Adding a couple more milliseconds to account for synaptic transmission, and taking as the period of the oscillation 250 ms (recall the SWD frequency of ~4 Hz), it is estimated a theoretical possible phase lag between 3 and 5 ms (4 and 7°, or 0.07–0.12 rad). Thus, some of the phase lag we observe in the recordings and also determine from the linear stability

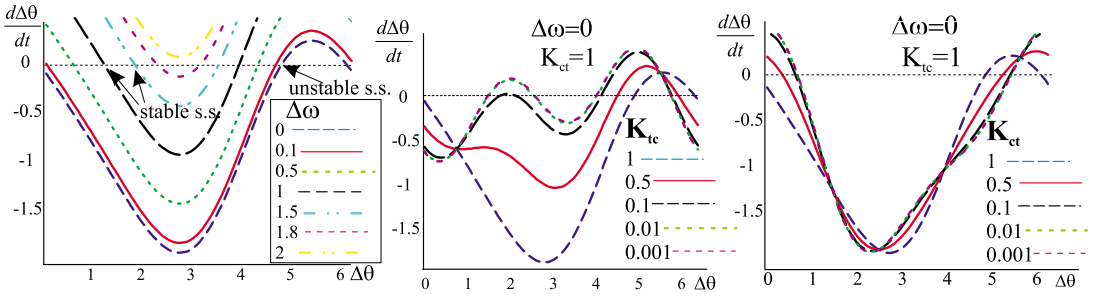


FIG. 5. (Color online) Changes in the stable phase differences brought about by differences in intrinsic frequencies and coupling factors. Steady states (SSs) are found in the crossing of the graph with $\frac{d\Delta\theta}{dt}=0$, and are stable if slopes are negative. Left, for symmetric coupling ($K_{tc}=K_{ct}=1$), increasing the difference in intrinsic frequencies ($\Delta\omega$) results in larger phase differences values for the stable fixed point and eventual vanishing of the stable state (for $\Delta\omega=2$, yellow line). Middle, decreasing the thalamo-cortical coupling ($K_{tc}$) while keeping $K_{ct}=1$, results in little change to the first stable fixed point and the apparition of a second (around 2.5 rad, which is never observed experimentally). Colors represent $K_{tc}$ values of blue, 1; red, 0.5; black, 0.1; green, 0.01; magenta, 0.001. Increasing the frequency difference in this case results in similar observation as in the previous case: shift of the curve upwards and eventual disappearance of the fixed points (Table I). Third panel, decreasing the cortico-thalamic coupling ($K_{ct}$) while keeping $K_{tc}=1$ results in the shift to the left of the stable phase difference ($<1$ rad). Colors represent $K_{ct}$ values.

analysis aforementioned, can be due to conduction and synaptic delays in the transmission between these two brain areas. We note that the calculated unstable fixed points aforementioned (4.18 rad, which would appear in the recording almost as antiphase) are never found in the experimental recordings of SWD, as suggested by the "unstable" nature derived from the model.

To determine the relative stability of the phase differences with different oscillating frequencies, further analysis was done by letting $\Delta\omega$ change from 0 to an arbitrary large value. As can be seen in the plots in Fig. 5, left panel, the stable state becomes larger and disappears when differences in intrinsic frequency are typically $>1.9$, if coupling is symmetric ($K_{tc}=K_{ct}$). Considering now asymmetric coupling, and taking a value of 1 as the maximum coupling factor, it can be seen (Fig. 5) that changing the thalamo-cortical coupling ($K_{tc}$) while maintaining constant the cortico-thalamic ($K_{ct}$) results in very little change in the stable steady state at around 6 rad, if $\Delta\omega=0$ as shown in Fig. 5 middle plot (increasing $\Delta\omega$ only displaces the graphs upwards, meaning that the stationary states will disappear as shown on the left panel of the figure). As $K_{tc}$ decreases relative to $K_{ct}$ there appears an additional stable stationary state (at around $\sim 2.1-2.6$ rad). This indicates that bistability may be possible in the system, and adds further evidence for possible multistable phenomena in nervous system function [15]. Numerical values are summarized in Table I. If $K_{ct}$ is decreased while $K_{tc}$ is held constant, as depicted in the right panel of Fig. 5, the stationary state appears at small phase values ($<0.8$ rad) as $K_{ct}$ values become smaller (see Table II for numerical details).

A look at the values of the stable phase differences presented in Tables I and II suggests that the thalamo-cortical coupling ($K_{tc}$) keeps the oscillation more "tightly controlled," because there are small changes to the fixed point when the cortico-thalamic coupling is decreased relative to the thalamo-cortical even for $\Delta\omega>1.8$ (Table II). On the other hand, there are substantial variations in the fixed point as the thalamo-cortical coupling becomes smaller (Table I). The data in those tables can also be visualised as an Arnold tongue for 1:1 locking, where we note that $\Delta\omega$ has to be larger for the fixed point to disappear when the thalamo-cortical coupling is dominant: for $\Delta\omega=1.8$ there is still a fixed point for all coupling values, in Table II. A graph representing the 1:1 locking for values of the couplings and frequency differences is shown in Fig. 6. Neurophysiological data demonstrated that thalamo-cortical synapses are stronger (in that these are more effective to drive the cortical cells) than cortico-cortical by a factor of 4.8 [26], thus sup-

TABLE I. Variations in the stable phase difference (in radians) by changes in thalamo-cortical coupling ($K_{tc}$) and in intrinsic frequency differences ($\Delta\omega$). The cortico-thalamic coupling ($K_{ct}$) was set to 1. Note that two stable fixed points appear for low values of coupling and intrinsic frequency difference ($\Delta\omega=0$).

| $K_{tc}$ | $\Delta\omega=0$ | $\Delta\omega=0.5$ | $\Delta\omega=1$ | $\Delta\omega=1.2$ | $\Delta\omega=1.5$ |
|---|---|---|---|---|---|
| 1 | 6.18 | 0.61 | 1.23 | 1.48 | 1.86 |
| 0.5 | 5.82 | 0.26 | 2.7 | | |
| 0.1 | 2.04/5.7 | 6.2 | | | |
| 0.01 | 2.5/5.66 | 6.12 | | | |
| 0.001 | 2.53/5.65 | 6.11 | | | |

TABLE II. Variations in the stable phase difference (in radians) by changes in cortico-thalamic coupling ($K_{ct}$) and in intrinsic frequency differences ($\Delta\omega$). The thalamo-cortical coupling ($K_{tc}$) was set to 1.

| $K_{ct}$ | $\Delta\omega=0$ | $\Delta\omega=0.5$ | $\Delta\omega=1$ | $\Delta\omega=1.8$ | $\Delta\omega=1.91$ |
|---|---|---|---|---|---|
| 1 | 6.18 | 0.606 | 1.23 | 2.32 | 2.67 |
| 0.5 | 0.45 | 0.93 | 1.32 | 2.18 | |
| 0.1 | 0.715 | 1.05 | 1.36 | 2.05 | |
| 0.01 | 0.757 | 1.07 | 1.364 | 2.02 | |
| 0.001 | 0.761 | 1.071 | 1.365 | 2.02 | |

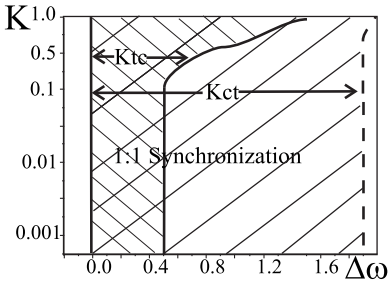


FIG. 6. Schematic representation of Tables I and II. Depicts the area of 1:1 frequency locking where stable phase differences appear (numerical values in the tables), and highlights the stronger influence of the thalamo-cortical coupling ($K_{tc}$), as the area of synchronization is larger regardless of how small $K_{ct}$ is (larger shaded area); note that the synchronized state is almost constant for varying $K_{ct}$. For $\Delta\omega > 2$ there is no stable 1:1 locking. In the figure, areas shaded and labeled $K_{tc}$ and $K_{ct}$ represent stable 1:1 locking when those couplings are changed and the other is kept constant. The $y$ axis (coupling) is logarithmic, to help visualization.

porting the concept of a stronger influence of the thalamic input to cortex (equivalently the thalamo-cortical coupling) in the stabilization of a phase locking pattern.

## IV. DISCUSSION

The results obtained indicate a good agreement between the phenomena observed experimentally and those extracted from the model, and suggest that this admittedly very simplistic model, can be the origin for further studies that can include the presence of noise and the stochastic analysis of the distribution of phase differences in brain recordings.

The SWD can be considered an asymptotic stable limit cycle [11] that when weakly perturbed can be reduced to a phase model [12]. To implement this, we exploit the PRC as a tool to understand coordinated brain activity. The PRC represents a natural approach to characterize interactions [3,14,16]. Within the framework of coupled oscillator theory, PRCs have been used to analyze synchronization properties of natural [18–21] and artificial neural systems [22]. In general, coupled oscillator theory is based on weakly coupled oscillators [3,12,13], and rests upon two main characteristics: intrinsic oscillators that are weakly coupled. Whether or not these features are common to nervous systems is still debated, however, some reasonable approximations are useful to unravel the dynamics of neuronal coordinated activity [27,28]. Thus, as approximations in our study, we used as "intrinsic frequency" ($\omega$) the frequency of the SWD. This represents a sort of "functional" intrinsic frequency, because brain oscillations are not completely intrinsic considering that rhythms depend on input from other brain areas as much as on the intrinsic biophysical cellular properties. This is one reason why, depending on the specific brain state, a particular brain region will display different rhythms. We just note that classical synchronization theory distinguishes between mutual synchronization of self-sustained periodic oscillators, and forced synchronization by driving forces [28,29]. It seems more plausible, for studies involving nervous tissue, that forced synchronization is the main operant, while mutual synchronization is a more rare phenomenon. This is due to the strong influence that an area of synchronously firing cells has upon a receiving network, this influence would be closer to forcing. Mutual synchronization can take place in the case of cells coupled via gap junctions, for instance, where the interactions are relatively weak. SWDs can be treated as both mutual synchronization and as forced synchronization, for two main reasons. First, the influence of the thalamus on the cortex (and viceversa) can be considered strong in this type of paroxysmal (seizure) activity because there are many cells firing (almost) synchronously and thus providing strong synaptic input to the receiver neuronal ensemble; indeed, the fact that a single pulse to the thalamus or to the cortex triggers a SWD (Fig. 2 and Ref. [24]) is an indication of the strength of the coupling between these areas and that any of these two areas can be the generators of the seizure. Second, there is an ongoing very periodic oscillation in thalamus and cortex, represented as SWD in field potential recordings, that provide the opportunity for fine adjustment of frequencies characteristic of mutual synchronization [25,29].

Another approximation we introduce is that we use the PRC as the interaction function $H(\Delta\theta)$. This is reasonable in our case because we recorded the activity in one brain area while perturbing the other, connected synaptically to the first one. Hence, in this case, the change in the SWD derived from the local field potentials in the cortex, for instance, represents the "interaction" between the local perturbation by our stimulus in the thalamus and the synaptic input generated by thalamic axons in the cortex. In addition, the synaptic inputs are very fast compared with the period of the oscillation ($\sim$250 ms). Therefore, our PRC naturally includes the convolution of the perturbation and the synaptic input, and for this reason we do not need to convolve the PRC with the $\alpha$ function (representing the synaptic potential), as is the normal approach in other studies where the perturbation is applied directly to the cell or brain area in question [18,20]. Our experimental approach has the additional advantage of allowing a more realistic input to each brain area, in that the cortex (thalamus) receives the result of the applied stimulus via "real" synaptic potentials in the thalamic (cortical) axons. As Oprisan *et al.* [30] recommended: "The perturbation used to generate the PRC must resemble as closely as possible the input that the oscillator would receive in the circuit." A final approximation is that we consider two brain areas that are not as homogenous as we may desire. Indeed, the input from the cortex is not only arriving to the sensory (relay) thalamic nuclei, but also importantly to the thalamic reticular nucleus, which is comprised of inhibitory cells which in turn synapse onto thalamic relay cells. Therefore a more accurate model would consist of three interconnected areas: cortex, relay thalamic nuclei, and reticular nucleus.

The model we used is based on the classical Kuramoto model [13], which has been widely used to examine the onset and characteristics of synchronization in many systems. One limitation is that the natural frequencies and coupling factors are fixed, rather than variable as they normally are in nervous system activity where frequencies and coupling are changing at all time scales. In this regard, the approaches that include time varying frequencies and couplings in generali-

zations of the Kuramoto model are promising [31,32]. Additional refinements may include the incorporation of the dynamics in the neuronal dendrites [33].

The PRCs we found in our experiments, indicating that the effects of the perturbation tend to be the advancement of the cycle, are obviously founded in the physiological characteristics of the circuitries involved. The advancement (or "excitation") of the cortical activity in response to thalamic stimulation (positive values in Fig. 3) can be expected if we consider the phenomenon known as the "thalamic augmenting response" [34]. In this phenomenon, the net result of thalamic inputs to cortex will be an enhancement of the cortical excitation. On the other hand, the thalamic PRC in response to cortical stimulation advances the signal only for some stimulation phases, not changing or even delaying the signal for other stimulation phases (Fig. 3), which may reflect the "inhibitory dominance" of cortical inputs to thalamus [10]. This phenomenon resides in the fact that, as aforementioned, the cortex stimulates the thalamic relay cells as well as the inhibitory reticular neurons, and these cells then provide a strong inhibitory component to the thalamic relay cells. Hence, considering first the summation, in the thalamic relay cell, of the strong inhibitory potentials from the reticular cells and the excitatory potentials from the cortical cells, which results in a net long-lasting inhibitory potential [10], and second, the intrinsic cellular properties of the thalamic neurons which will promote a calcium spike in response to inhibition (the so-called rebound low-threshold calcium spike), then the effect of the cortical perturbation will be different depending upon the time (phase) of the perturbation: we can conceive that some phases will promote excitation (and hence advancement) because of the calcium spike in response to the inhibitory potential from the reticular cells, while other phases will result in the inhibitory potential retarding the next wave.

The model constructed so far can predict the phase difference that we normally observe in our recordings. Thus, while very simple, this initial model captures some properties of the thalamocortical activity. Similar stable phase differences that are not perfectly in-phase, and unstable phase differences as well, have been found recently using a related model based on a simulation of a seizure model [35]. The phase lag can be due to conduction delays, nevertheless in spite of conduction (propagation) delays that will cause phase dispersion, close to zero-phase locking has been identified in vivo using field potential recordings [36]. We note that the oscillator (thalamo-cortical SWD) relaxes rapidly to the limit cycle after perturbation [Fig. 2(b)], similar to the activity of the cardiac oscillator studied by Glass *et al.* [37], hence it is conceivable that the dynamics of thalamo-cortical activity can be approximated by circle maps. We are currently using these maps to study other frequency locking ratios because, even though we have seen only the 1:1 locking in these recordings from rats, there is indication of multiple locking in human absence seizures [38]. In addition, conceptually similar studies have been carried out in the cardiac system, and the derivation of one-dimensional maps from the experimental manipulations can provide information regarding multistability and dynamical bifurcations [39]. From our perspective, this type of models also allow further improvements that will take into consideration the role of fluctuations in neuronal dynamics, thus, the stochastic approach based on Langevin and Fokker-Planck equations represents a logical extension of these studies.

In conclusion, our observations and those of others support the notions of multistability in nervous system function that can be derived from coupled oscillator models [33,35], and indicate that metastability is a fundamental property of brain dynamics [15,27,40,41]. As a complement to empirical observations, the frameworks of nonlinear dynamical systems and coupled oscillator theory formulations allow a deeper understanding of the coordinated activity in complex systems, and will provide fundamental insight into brain function.

## ACKNOWLEDGMENTS

Our research is supported by a Discovery grant from the Natural Sciences and Engineering Research Council of Canada (NSERC).

[1] W. Singer, NeuroQuantology **4**, 134 (2006).
[2] S. L. Bressler and J. A. S. Kelso, Trends Cogn. Sci. **5**, 26 (2001).
[3] A. Winfree, *The Geometry of Biological Time* (Springer Verlag, Berlin, 1980).
[4] M. Breakspear, Neuroinformatics **2**, 205 (2004).
[5] K. J. Friston, Neuroscientist **7**, 406 (2001).
[6] D. Smirnov, B. Bezruchko, and Y. Seleznev, Phys. Rev. E **65**, 026205 (2002).
[7] B. Bezruchko, T. Dakanev, and D. Smirnov, Phys. Rev. E **64**, 036210 (2001).
[8] R. Friedrich, S. Siegert, J. Peinke, St. Luck, M. Siefert, M. Lindemann, J. Raethjen, G. Deuschl, and G. Pfister, Phys. Lett. A **271**, 217 (2000).
[9] O. C. Snead, Epilepsia **29**, 361 (1988).
[10] A. Destexhe, D. Contreras, and M. Steriade, J. Neurophysiol. **79**, 999 (1998).
[11] J. Hernandez, P. Valdes, and P. Villa, NeuroReport **7**, 2246 (1996).
[12] F. C. Hoppensteadt and E. M. Izhikevich, *Weakly Connected Neural Networks* (Springer, Berlin 1997).
[13] Y. Kuramoto, *Chemical Oscillations, Waves, and Turbulence* (Springer, New York, 1984).
[14] N. Kopell and G. B. Ermentrout, J. Math. Biol. **90**, 87 (1988).
[15] J. A. S. Kelso, *Dynamic Patterns: The Self-organization of Brain and Behaviour* (MIT, Cambridge, 1995).
[16] T. Pavlides, *Biological Oscillators: Their Mathematical Analysis* (Academic Press, New York, 1973).
[17] J. Rinzel and G. B. Ermentrout, in *Methods in Neuronal Modeling*, edited by C. Koch and I. Segev (MIT, Cambridge,

1989).
[18] P. Goel and B. Ermentrout, Physica D **163**, 191 (2002).
[19] T. Netoff, M. Banks, A. Dorval, C. Acker, J. Haas, N. Kopell, and J. White, J. Neurophysiol. **93**, 1197 (2005).
[20] R. F. Galán, G. B. Ermentrout, and N. N. Urban, Phys. Rev. Lett. **94**, 158101 (2005).
[21] R. F. Galán, G. B. Ermentrout, and N. N. Urban, Neurocomputing **69**, 1112 (2006).
[22] S. Oprisan and C. Canavier, Neural Comput. **14**, 1027 (2002).
[23] W. Govaerts and B. Sautois, Neural Comput. **18**, 817 (2006).
[24] E. Proulx, Y. Leshchenko, L. Kokarovtseva, V. Khokhotva, M. El Beheiry, O. C. Snead, and J. L. Perez Velazquez, Eur. J. Neurosci. **23**, 489 (2006).
[25] A. Pikovsky, M. Rosemblum, and J. Kurths, *Synchronization: A Universal Concept in Nonlinear Sciences* (Cambrige University Press, Cambridge, 2001).
[26] Z. Gil, B. W. Connors, and Y. Amitai, Neuron **23**, 385 (1999).
[27] J. L. Perez Velazquez, Physica D **212**, 161 (2005).
[28] J. L. Perez Velazquez, NeuroQuantology **4**, 155 (2006).
[29] V. S. Anishchenko, V. V. Astakhov, A. B. Neiman, T. E. Vadivasova, and L. Schimansky-Geier, *Nonlinear Dynamics of Chaotic and Stochastic Systems* (Springer, Berlin, 2002).
[30] S. Oprisan, V. Thirumalai, and C. Canavier, Biophys. J. **84**, 2919 (2003).
[31] D. Cumin and C. Unsworth, Physica D **226**, 181 (2007).
[32] Y. L. Maistrenko, B. Lysyansky, C. Hauptmann, O. Burylko, and P. A. Tass, Phys. Rev. E **75**, 066207 (2007).
[33] M. Majtanik, K. Dolan, and P. Tass, J. Biol. Phys. **32**, 307 (2006).
[34] R. S. Morison and E. W. Dempsey, Am. J. Physiol. **138**, 297 (1943).
[35] D. Takeshita, Y. Sato, and S. Bahar, Phys. Rev. E **75**, 051925 (2007).
[36] W. J. Freeman, G. Gaal, and R. Jorsten, Int. J. Bifurcation Chaos Appl. Sci. Eng. **13**, 2845 (2003).
[37] L. Glass, M. R. Guevara, A. Shrier, and R. Perez, Physica D **7**, 89 (1983).
[38] J. L. Perez Velazquez, L. Garcia Dominguez, and R. Wennberg, Phys. Rev. E **75**, 011922 (2007).
[39] A. R. Yehia, D. Jeandupeux, F. Alonso, and M. R. Guevara, Chaos **9**, 916 (1999).
[40] J. L. Perez Velazquez and R. Wennberg, in *Recent Research Developments in Biophysics* (Transworld Research Network, Kerala, 2004), Vol. 3.
[41] A. A. Fingelkurts and A. A. Fingelkurts, Int. J. Neurosci. **114**, 843 (2004).